ISSN 0022-4766, Journal of Structural Chemistry, 2021, Vol. 62, No. 11, pp. 1801-1809. © Pleiades Publishing, Ltd., 2021.
Russian Text © The Author(s), 2021, published in Zhurnal Strukturnoi Khimii, 2021, Vol. 62, No. 11, pp. 1913-1920.

THE SYNTHESIS AND PROPERTIES OF A SODIUM SUPRAMOLECULAR CRYSTAL NETWORK CONSTRUCTED WITH FUNCTIONAL PYRAZINE SULFONIC ACID*

Y.-J. Liang[1], D. Hu[2], L. Zhang[1], Y. Jiang[3], and J.-X. Li[4]*

Sulfonic acid groups with C_{3v} symmetry can coordinate with metal ions to produce multidimensional structures due to their flexible coordination modes. They can also penetrate into supramolecular structures through an intriguing bridging pattern and weak interactions. Herein, a novel heterocyclic sodium sulfonate supramolecular structure, namely $[Na(Pyr\text{-}SO_3)(H_2O)]_n$ where $Pyr\text{-}SO_3H$ is pyrazine sulfonic acid, is synthesized by utilizing $NaBF_4$ to coordinate with the $P–SO_3H$ ligand through the solvent evaporation method. The single crystal X-ray diffraction (XRD) data indicate that the as-formed structure belongs to the *Pbca* space group. Additional properties are characterized by powder XRD, thermal analysis, and solid-state fluorescence. In particular, the introduction of a soft alkali metal ion can coordinate with the oxygen atom of the sulfonate ligand and form a Na–O bridging configuration that can not only significantly improve the pyrazine sulfonic acid ligand coordination ability, but also provide a reference for the extended study of functional sulfonate polymers in the future.

DOI: 10.1134/S0022476621110172

Keywords: metal-organic architecture, pyrazine sulfonate, alkali metal, bridging pattern, supramolecular structure.

INTRODUCTION

In recent years, the synthesis, structural modifications, and physicochemical properties of metal-organic based architectures have received considerable attentions not only because of their diverse structures [1, 2], but also their promising applications in many areas, such as proton conduction [3], nonlinear optical materials [4], magnetism [5, 6], catalysis [7], ion recognition and exchange [8, 9], chemical sensing [10, 11], luminescence [12, 13], biomedicine [14], and so on. Among them, the sulfonate group has recently received much attention for its useful features, such as flexible coordination modes,

[1]School of Medicine, Foshan University, Foshan, People′s Republic of China. [2]Department of Ophthalmology, No. 1 People's Hospital of Foshan, People′s Republic of China. [3]School of Chemistry and Chemical Pharmaceutical Science, Guangxi Normal University, Guilin, People′s Republic of China. [4]Henan Key Laboratory of Function-Oriented Porous Materials, College of Chemistry and Chemical Engineering, Luoyang Normal University, Luoyang, People′s Republic of China; *ljx6281@126.com. Original article submitted April 15, 2021; revised June 13, 2021; accepted July 12, 2021.

* Supplementary materials are available for this article at doi 10.1134/S0022476621110172 and are accessible for authorized users.

binding preferences to metal ions, and widely bridging extension [15, 16]. For instance, Wu and co-workers [17] used phenyl sulfonic acid, *p*-aminobenzene sulfonic acid, and *p*-methylbenzene sulfonic acid to synthesize three Co(II) coordination complexes under hydrothermal conditions. They found that the formation of hydrogen bonds and π–π stacking interactions can organize the architecture into a 3D supramolecular topology by connecting discrete molecules. In addition, Stock et al. [18] employed a novel linker molecule that contained both phosphonic and sulfonic acid groups to prepare four new coordination polymers using high-throughput methods. Interestingly, water sorption measurements confirmed that the synthesized framework polymers were potentially porous. Just recently, the Li group [19] chose sulfo-functionalized aromatic carboxylic acid ligands to construct three new Cu(II) coordination complexes. The resulting polymers exhibit distinct proton conductivity properties and photocatalytic activities that could be suitable for the development of functionalized sulfonate-based photocatalytic and proton conductivity coordination complexes.

Nevertheless, the study of heterocyclic sulfonates coordinated with metal ions remains a challenging task. Sulfonic acid ligands exhibit relatively weak coordination abilities and a spatially diverse structural motif during the coordination process, as presented by *M*···*M*, *M*···C, *X*–H···*M*, or *M*···π interactions, where *M* stands for metal ions [20, 21]. The previously mentioned factors may contribute to the final structure formation and polymer properties, as well as an increase in potential applications of heterocyclic sulfonate-based polymers. Our previous experiments successfully produced two silver-based supramolecular structures and a 3D Cu(II) sulfonate polymer; the results indicated that they might have potential in optical sensing and biomedical applications [22, 23].

It is worth noting that alkali and alkaline earth metals can produce stable complexes with high performance [24, 25]. In particular, the sodium ion exhibits a much greater tendency to coordinate with sulfonate ligands compared to transition metal ions. The radius and charge density of sodium ions may affect the hydration energy and compatibility with sulfonate anions, resulting in a greater affinity for the sulfonate ligand during the coordination process [26]. Taking into account the importance of sodium ions in biomedicine, especially the participation in a range of physiological processes, herein, we employed sodium ions and Pyr-SO_3H to design and synthesize the Na^+ polymer. The as-prepared polymer is characterized by IR spectroscopy, elemental analysis, and X-ray crystallography. Moreover, the thermal stability and solid-state fluorescent properties are also investigated. We hope that these results will provide a solid foundation for the extended study of sulfonate-based functional polymers in the future.

EXPERIMENTAL

Materials and methods. All the reagents were of analytical grade and used as received without further purification. Notably, the detailed preparation of the ligand, namely pyrazine sulfonic acid (Pyr-SO_3H), can be found in our previous publication [27].

Preparation and characterization of [Na(Pyr-SO_3)(H_2O)]$_n$. Typically, $NaBF_4$ (0.3 mmol) and the ligand, pyrazine sulfonic acid (Pyr-SO_3H, 0.2 mmol), were mixed with solvents, which included THF, methanol, and acetonitrile, in a certain proportion (1:3:1). Subsequently, the mixture was placed in the water bath and stirred at 60 °C for 6 h. Finally, the filtrate was allowed to evaporate at room temperature in a natural way to get the cube-like crystal after 24 days. Yield 68% (based on Na). Notably, the IR spectrum was recorded on the FTIR spectrometer (PE Spectrum One, USA) with KBr as the substrate, and the thermogravimetric analysis was conducted (Labsys Evo-TGA, France). The solid-state fluorescence characterization was carried out using a HORIBA JOBIN JVON fluorescence spectrophotometer (FL3-P-TCSPC). The powder of the pyrazine sulfonic acid ligand and as-synthesized [Na(Pyr-SO_3)(H_2O)]$_n$ were placed in quartz slides for observation respectively, and the fluorescence spectra were obtained by scanning at a 3 nm slit width at room temperature. Anal. calcd for $C_4H_5N_2NaSO_4$ (%): C 24.00, H 2.52, N 14.03. Found (%): C 24.38, H 2.89, N 14.24. IR spectra (Supplementary Materials) (KBr, cm^{-1}): 3446 vs, 1621 vs, 1516 s, 1426 w, 1385 s, 1242 m, 1223 w, 1144 s, 1062 m, 859 vs, 728 vs.

X-ray crystallography. The X-ray diffraction data for as-synthesized [Na(Pyr-SO_3)(H_2O)]$_n$ were collected at 298 K using the Agilent Super-Nova diffractometer (MoK_α, λ = 0.071073 nm). Related crystal data were solved with the Olex2

software [28]. Notably, the direct method and the full matrix least-squares method within the SHELXTL program package were used to solve and determine the structure, respectively. Furthermore, all non-hydrogen atoms were used with the anisotropic thermal parameters [29]. All the non-hydrogen atoms were refined anisotropically. The hydrogen atoms were generated geometrically and treated by a mixture of independent and constrained refinements. Crystallographic data are listed in Table 1; the selected bond distances and angles are presented in Table 2; the hydrogen bonds can be seen in Table 3.

TABLE 1. Crystal Data and Structure Refinement for $[Na(Pyr\text{-}SO_3)(H_2O)]_n$

Empirical formula	$C_4H_5N_2NaO_4S$
Formula weight	200.15
Wavelength, Å	0.71073
Crystal system	Orthorhombic
Space group	*Pbca*
a, *b*, *c*, Å	8.17414(19), 11.7287(3), 15.7452(3)
V, Å^3	1509.52(6)
Z	8
Calculated density, g/cm^3	1.761
Absorption coefficient, mm^{-1}	0.459
F(000)	816.0
Crystal size, mm	0.40×0.20×0.12
2θ range for data collection, deg	6.604 to 52.74
Reflections collected	14339
Unique data	1541
R_{int}	0.0431
Completeness to θ, %	100
Refinement method	Full-matrix least-squares on F^2
Data / restraints / parameters	1541 / 0 / 117
GOOF on F^2	1.128
Final *R* indices ($I > 2\sigma(I)$)	$R_1 = 0.0322$, $wR_2 = 0.0842$
R indices (all data)	$R_1 = 0.0345$, $wR_2 = 0.0858$
Largest diff. peak / hole, e/Å^3	0.25 / –0.50

TABLE 2. Selected Bond Distances and Bond Angles of $[Na(Pyr\text{-}SO_3)(H_2O)]_n$

Bond length	Distance, Å	Bond length	Distance, Å
Na1–O4$^{\#1}$	2.3792(15)	Na1–Na1$^{\#1}$	3.7111(14)
Na1–O3$^{\#2}$	2.3945(16)	O1–Na1$^{\#5}$	2.4594(14)
Na1–O2	2.4400(13)	O3–Na1$^{\#6}$	2.3945(16)
Na1–O1$^{\#3}$	2.4594(14)	O4–Na1$^{\#1}$	2.3791(15)
Na1–O4	2.4899(16)	N2–Na1$^{\#7}$	2.5270(17)
Bond angle	Value, deg	Bond angle	Value, deg
1	2	3	4
O4$^{\#1}$–Na1–O3$^{\#2}$	106.01(6)	O3$^{\#2}$–Na1–Na1$^{\#1}$	147.08(6)
O4$^{\#1}$–Na1–O2	161.80(6)	O2–Na1–Na1$^{\#1}$	120.77(4)
O3$^{\#2}$–Na1–O2	91.09(6)	O1$^{\#3}$–Na1–Na1$^{\#1}$	85.54(4)
O4$^{\#1}$–Na1–O1$^{\#3}$	82.16(5)	O4–Na1–Na1$^{\#1}$	39.25(3)
O3$^{\#2}$–Na1–O1$^{\#3}$	95.99(5)	N2$^{\#4}$–Na1–Na1$^{\#1}$	94.77(5)

TABLE 2. (Cont.)

1	2	3	4
O2–Na1–O1$^{\#3}$	102.60(5)	S1–O1–Na1$^{\#5}$	123.22(8)
O4$^{\#1}$–Na1–O4	80.71(6)	S1–O2–Na1	147.28(8)
O3$^{\#2}$–Na1–O4	171.00(6)	S1–O3–Na1$^{\#6}$	173.77(11)
O2–Na1–O4	81.66(5)	Na1$^{\#1}$–O1–Na1	99.29(6)
O1$^{\#3}$–Na1–O4	90.82(5)	Na1$^{\#1}$–O4–H4A	137.8(19)
O4$^{\#1}$–Na1–N2$^{\#4}$	91.36(6)	Na1–O4–H4A	103(2)
O3$^{\#2}$–Na1–N2$^{\#4}$	78.27(5)	N1$^{\#1}$–O4–H4B	105(2)
O2–Na1–N2$^{\#4}$	85.96(5)	Na1–O4–H4B	108(2)
O1$^{\#3}$–Na1–N2$^{\#4}$	169.88(6)	C3–N2–Na1$^{\#7}$	118.79(12)
O4–Na1–N2$^{\#4}$	95.81(6)	C2–N2–Na1$^{\#7}$	124.68(12)
O4$^{\#1}$–Na1–Na1$^{\#1}$	41.46(4)		

Symmetry transformations used to generate equivalent atoms: $^{\#1}$ $-x+1, -y+1, -z+1$; $^{\#2}$ $x+1/2, -y+3/2, -z+1$; $^{\#3}$ $-x+3/2, y-1/2, z$; $^{\#4}$ $x, -y+3/2, z+1/2$; $^{\#5}$ $-x+3/2, y+1/2, z$; $^{\#6}$ $x-1/2, -y+3/2, -z+1$; $^{\#7}$ $x, -y+3/2, z-1/2$.

TABLE 3. Hydrogen Bond Geometries (Å, deg) *of* $[Na(Pyr\text{-}SO_3)(H_2O)]_n$

Donor–H···Acceptor	*d*(*D*–H)	*d*(H···*A*)	*d*(*D*···*A*)	∠(*D*H*A*)
O4–H4A···N1	0.83(3)	2.06(3)	2.877(2)	168(3)
O4–H4B···O2$^{\#1}$	0.77(3)	2.11(3)	2.864 (2)	165(3)

Symmetry code: $^{\#1}$ $x-1/2, -y+3/2, -z+1$.

RESULTS AND DISCUSSION

Structural description. Based on the single crystal X-ray diffraction (XRD) data, two sodium ions in the asymmetric unit are coordinated with oxygen and nitrogen atoms from the pyrazine sulfonic acid ligands to construct a distorted octahedral configuration (Fig. 1*a*). In the horizontal direction, two sodium ions are chelated with oxygen atoms of two water molecules to form a parallelogram configuration. The related bond lengths and angles are: Na1–O4$^{\#1}$, 2.379 Å; Na1–O4, 2.490 Å; Na1$^{\#1}$–O1–Na1, 99.29°; O4$^{\#1}$–Na1–O4, 80.71°. During the coordination process, Pry-SO_3 played the role of an uncoordinated counterbalancing anion and an anionic ligand. In fact, the distance between Na1$^{\#1}$ and Na1 was measured as 3.711 Å, and the bond lengths and angles mentioned above are consistent with the literature reports [30, 31]. Note that sodium atoms from the asymmetric unit of the molecule can chelate with oxygen atoms of water molecules and sulfonate to form the parallelogram in terms of the affinity, and then to create a repeating wavy-like 1D chain in the equatorial plane. Subsequently, these as formed Na–O bridging configurations further act as the filling layer to extend into a 2D plane (Fig. 1*b*). Moreover, numerous intramolecular hydrogen bonds that occur between sulfonic acid groups in the adjacent layers with lengths of O4–H4A···N1 2.864 Å and O4–H4B···O2$^{\#6}$ 2.877 Å can be found between the main frame of the as-formed complex and coordinated water molecules. As can be seen in Fig. 1*c*, the flexible sodium sulfonate frames functioning as pillars could combine with these hydrogen bonds to facilitate the formation of a 3D structure. It should be noted that the adjacent pyrazine rings have different orientations between each layer. In particular, the pyrazine rings are staggered during the layer-to-layer accumulation, so that two kinds of outward and inward orientations within the same layer were shown, then resulting in their function as novel pillars for the 3D architecture construction (Fig. 1*d*) [32, 33]. We speculate that these results may either be closely related to a change in reaction conditions during the coordination process (such as concentration, pH, etc.) or due to the coordination of nitrogen atoms on the pyrazine ring with sodium ions, thus leading to different molecular interactions. No matter what is the cause, the interesting accumulation pattern of pyrazine sulfonic acid ligands described herein should continue to be studied.

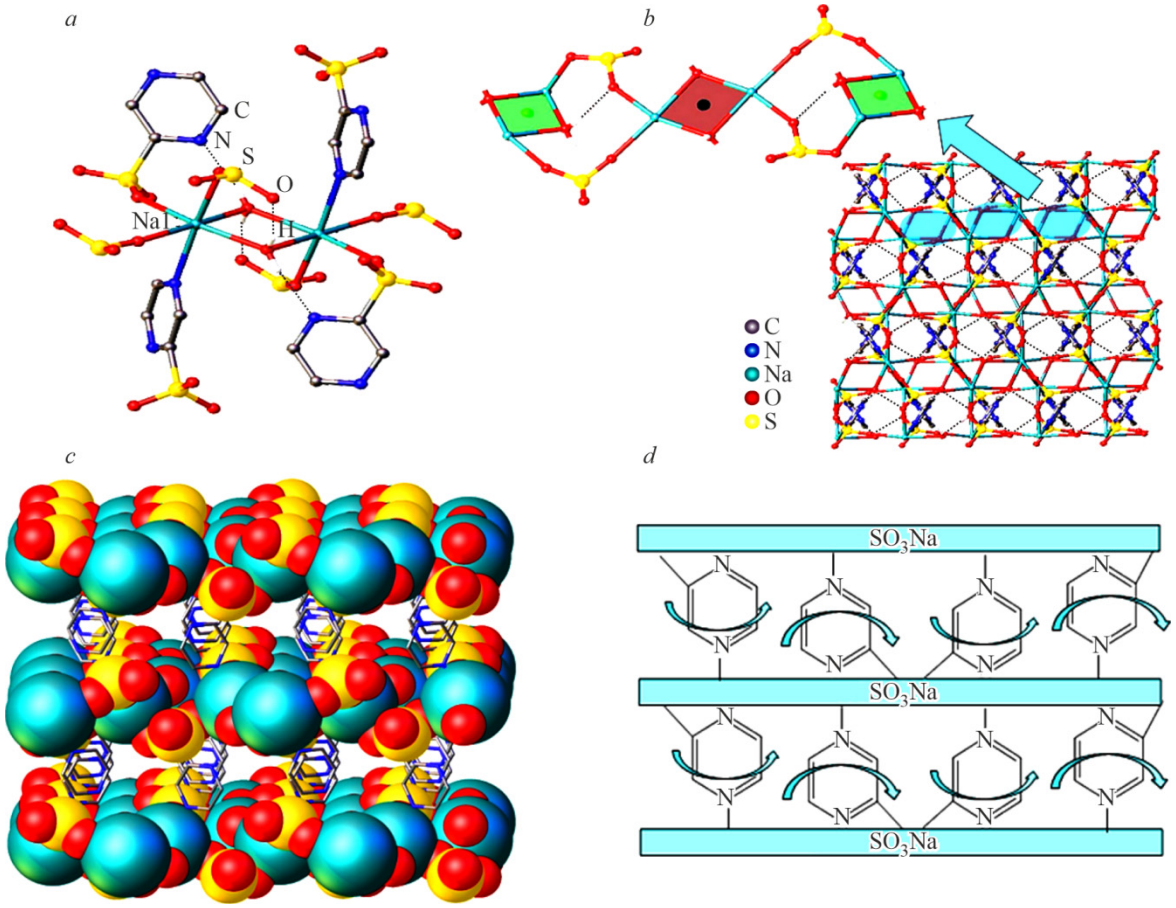

Fig. 1. Crystal structure of $[Na(Pyr\text{-}SO_3)(H_2O)]_n$. ($Pyr\text{-}SO_3H$ = pyrazine sulfonic acid): coordination environment of Na^+ ions (*a*), 2D framework of the interleaved lattice (*b*), 3D supramolecular structure with different packing patterns of $[Na(Pyr\text{-}SO_3)(H_2O)]_n$ (*c*), illustration of the rotation of pyrazine rings during the layer-to-layer accumulation (*d*).

Powder XRD. Fig. 2 shows the experimental and simulated powder XRD patterns of the polymer. Most of the peaks are observed to match the positions as their counterparts in the simulated part. However, a few peaks of the experimental powder XRD pattern in the angle range of 22-40° do not agree with the positions of the simulated pattern. We think that this can be ascribed to that the single crystal does not fully expose all its crystal faces during the powder XRD data collection. Therefore, the analysis and verification should be continued.

Thermal analysis. The thermal stability of $[Na(Pyr\text{-}SO_3)(H_2O)]_n$ could provide useful information in the development of additional applications. TGA of the polymer was performed from ambient temperatures to 600 °C with a heating rate of 10 °C/min and under the continuous N_2 flow. As shown in Fig. 3, the weight loss of $[Na(Pyr\text{-}SO_3)(H_2O)]_n$ was initially observed at approximately 140 °C, which was attributed to the release of water molecules. The observed weight loss percentage was 10.2% versus a theoretical value of 9.0%. The polymer framework decomposed rapidly on continuous heating, and the maximum weight loss appeared at approximately 400 °C. (The observed weight loss percentage was 82.3% versus a calculated value for the Na_2O substance of 84.5%.) Due to the obvious inflection point, we attributed the weight loss to pyrolysis of the sulfonic acid ligand. As the temperature increased further, the degradation rate of the polymer decreased until the pyrolysis residue as exhibited at approximately 600 °C (Obs. 7.6%, calcd 7.1%).

Luminescence. The solid-state fluorescence spectra of the sulfonate ligand and $[Na(Pyr\text{-}SO_3)(H_2O)]_n$ were recorded at room temperature. As shown in Fig. 4, at an excitation wavelength of 378 nm, the maximum emission signal of $[Na(Pyr\text{-}SO_3)(H_2O)]_n$ was detected at 450 nm. In particular, the fluorescence peaks of the polymer were weaker than those of the

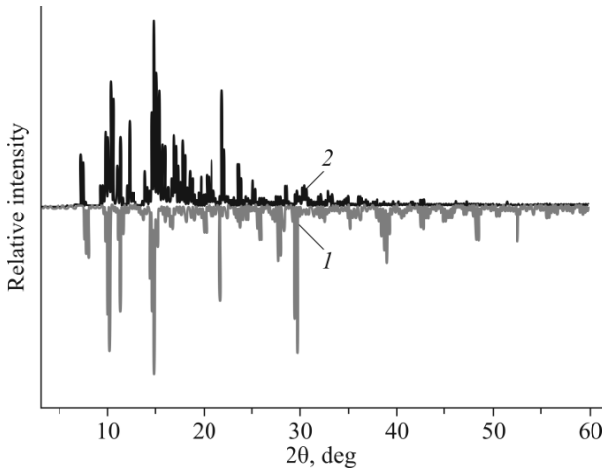

Fig. 2. Experimental (*1*) and simulated (*2*) powder XRD patterns of $[Na(Pyr\text{-}SO_3)(H_2O)]_n$.

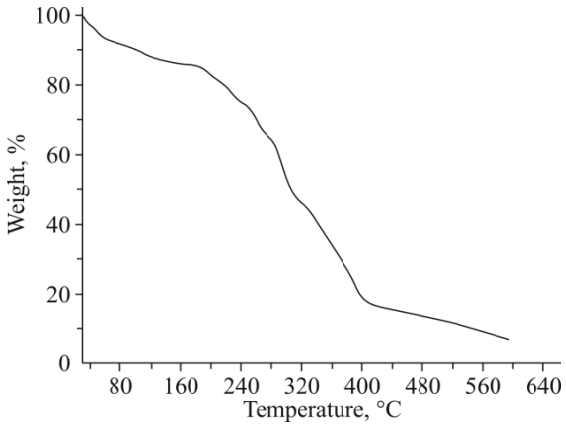

Fig. 3. TGA curve of $[Na(Pyr\text{-}SO_3)(H_2O)]_n$.

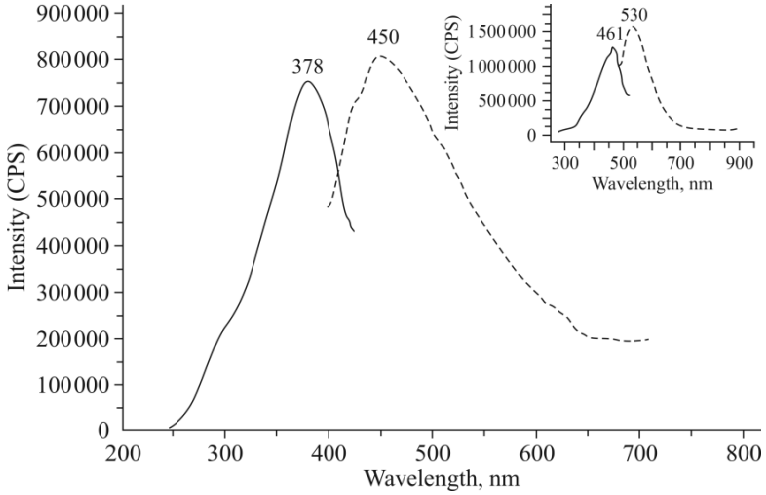

Fig. 4. Solid-state photoluminescence spectra of $[Na(Pyr\text{-}SO_3)(H_2O)]_n$ ($Pyr\text{-}SO_3H$ = pyrazine sulfonic acid). Note that solid line indicates the excitation wavelength and dotted line shows the emission signal of the polymer. Inset reports the solid-state photoluminescence spectra of the ligand, $PyrSO_3H$.

sulfonate ligand, and the maximum emission signal underwent a blue shift at approximately 80 nm compared to the ligand (λ_{ex} = 461 nm, λ_{em} = 530 nm). We attribute this to the coordination of Na^+ ions with the oxygen atoms of sulfonic acid and solvent molecules. This unique coordination structure reduces the number of degrees of freedom within the molecule and transfers energy. As a result, the existence of weak intermolecular interactions between Na^+ ions and the sulfonic acid ligand leads to a further increase in the HOMO–LUMO gap, which in turn leads to a certain degree of fluorescence quenching of the polymer [34-36]. Nevertheless, more analyses are needed to further support these results.

CONCLUSIONS

In summary, a sodium supramolecular crystal network, namely $[Na(Pyr\text{-}SO_3)(H_2O)]_n$ was successfully synthesized via the solvent evaporation method utilizing pyrazine sulfonic acid as the ligand. Although the sulfonate group has certain stretching and deformation characteristics, the highly symmetrical and rigid structure of the pyrazine ring largely restricts the variety of coordination modes and building blocks during the synthetic process. Alkaline metal ions have a strong oxygen affinity and easily form solvated hydrate ions with solvent molecules. Therefore, the introduction of softer alkali metal Na^+ ions allow them to function as bridging blocks and a good proton conductor to expand the 3D architecture of the polymer. Furthermore, Na^+ coordination with sulfonate groups might induce an increase in the HOMO–LUMO gap, thus leading to certain quenching of the polymer fluorescence intensity. We strongly believe that the polymer designed and constructed in this study is an excellent example of inorganic-organic hybrid materials which may provide a new method to explore the synthesis of supramolecular sulfonated pyrazine. A further study for the in vitro biomedical behavior of the as-prepared polymer is currently in progress.

ADDITIONAL INFORMATION

Supplementary data associated with the IR spectra of $[Na(Pyr\text{-}SO_3)(H_2O)]_n$ (Pyr-SO_3H = pyrazine sulfonic acid) can be found in the online version. The crystallographic data have been deposited with the Cambridge Crystallographic Data Center with CCDC deposition number 2076645. Copies of this information may be obtained free of charge from the CCDC, 12 Union Road, Cambridge, CB2 1EZ, UK (Fax: þ44 1223 336 033; E-mail: deposit@ccdc.cam.ac.uk or www.ccdc.cam.ac.uk).

ACKNOWLEDGMENTS

The research was supported by the National Key Research and Development Program of China (No. 2020YFC2004300), the Key Scientific Research Projects in Colleges and Universities of Henan province (No. 21A150036), the Science and Technology Key Project of Covid-19 in Foshan city (No. 2020001000206) and the Scientific Research Program of High-Level Talents of Foshan University (No. Gg07118).

CONFLICT OF INTERESTS

The authors declare that they have no conflict of interests.

REFERENCES

1. J. X. Li, Z. X. Du, L. Y. Xiong, L. L. Fu, and W. B. Bo. *J. Solid State Chem.*, **2021**, *293*, 121799. https://doi.org/10.1016/j.jssc.2020.121799
2. F. Wang, F. K. Tian, Y. X. Deng, L. L. Yang, H. H. Zhang, D. S. Zhao, B. Li, X. T. Zhang, and L. M. Fan. *Cryst. Growth Des*., **2021**, *21*, 4242-4248. https://doi.org/10.1021/acs.cgd.1c00479

3. B.-X. Han, Y-F. Jiang, X-R. Sun, Z-F. Li, and G. Li. *Coord. Chem. Rev*., **2021**, *432*, 213754. https://doi.org/10.1016/j.ccr.2020.213754
4. L. Zhang, H. J. Li, H. J. He, Y. Yang, Y. J. Cui, and G. D. Qian. *Small*, **2021**, *17*, 2006649. https://doi.org/10.1002/smll.202006649
5. J.-X. Li, Z.-X. Du, and W.-P. Huang. *Synth. React. Inorg. Met.-Org. Chem*., **2014**, *44*, 352-357. https://doi.org/10.1080/15533174.2013.769588
6. J. X. Li, Z. X. Du, L. L. Zhang, D. L. Liu, and Q. Y. Pan. *Inorg. Chim. Acta*, **2020**, *512*, 119890. https://doi.org/10.1016/j.ica.2020.119890
7. S. X. Li, P. Luo, H. Z. Wu, C. H. Wei, Y. Hu, and G. L. Qiu. *ChemCatChem*, **2019**, *11*(13), 2978-2993. https://doi.org/10.1002/cctc.201900199
8. J. X. Li and Z. X. Du. *J. Coord. Chem*., **2016**, *69*, 2563-2572. https://doi.org/10.1080/00958972.2016.1216106
9. J. F. Olorunyomi, T. Y. Liu, C. K. Ho, C. Y. V. Li, and K. Y. Chan. *Sep. Purif. Technol*., **2021**, *260*, 118219. https://doi.org/10.1016/j.seppur.2020.118219
10. J. X. Li, Z. X. Du, Q. Y. Pan, L. L. Zhang, and D. L. Liu. *Inorg. Chim. Acta*, **2020**, *509*, 119677. https://doi.org/10.1016/j.ica.2020.119677
11. J. X. Li, Z. X. Du, and X. Feng. *Z. Naturforsch., B*, **2019**, *74*(11/12), 833-838. https://doi.org/10.1515/znb-2019-0128
12. J. X. Li, Z. X. Du, J. Wang, and X. Feng. *Z. Naturforsch., B*, **2019**, *74*(11/12), 839-845. https://doi.org/10.1515/znb-2019-0147
13. J. X. Li and Z. X. Du. *J. Clust. Sci*., **2020**, *31*, 507-511. https://doi.org/10.1007/s10876-019-01666-w
14. G. Psomas. *Coord. Chem. Rev*., **2020**, *412*, 213259. https://doi.org/10.1016/j.ccr.2020.213259
15. H. Zhang, Z.-A. Yan, Z.-M. Wu, Z.-Q. Lin, W.-M. Liao, and J. He. *J. Solid State Chem*., **2020**, *287*, 121325. https://doi.org/10.1016/j.jssc.2020.121325
16. X. Tan, P. Sudarsanam, J. Tan, A. Wang, H. Zhang, H. Li, and S. Yang. *J. Environ. Chem. Eng*., **2020**, 104719. https://doi.org/10.1016/j.jece.2020.104719
17. Y. T. Wang, G. M. Tang, and Y. S. Wu. *Appl. Organomet. Chem*., **2020**, *34*, e5542. https://doi.org/10.1002/aoc.5654
18. S. Wöhlbrandt, A. Igeska, E. S. Grape, S. Øien-Ødegaard, A. Ken Inge, and N. Stock. *Dalton Trans*., **2020**, *49*, 2724. https://doi.org/10.1039/C9DT04571F
19. H.-G. Yu, B. Li, S. Liu, C. Jiang, Y.-S. Li, Y.-P. Wu, J. Zhao, and D-S. Li. *J. Solid State Chem*., **2021**, *294*, 121860. https://doi.org/10.1016/j.jssc.2020.121860
20. M. Li, H. Song, and B. Wang. *Organometallics*, **2015**, *34*, 1969. https://doi.org/10.1021/acs.organomet.5b00214
21. P. Godlewska, J. Hanuza, E. Kucharska, P. Solarz, S. Roszak, S. M. Kaczmarek, G. Leniec, M. Ptak, M. Kopacz, and K. Hermanowicz. *J. Mol. Struct*., **2020**, *1219*, 128504. https://doi.org/10.1016/j.molstruc.2020.128504
22. H. Hu, J. Quan, Z. Tan, J.-H. Fu, Y.-J. Liang, and J.-X. Li. *Russ. J. Gen. Chem*., **2021**, *91*, 910-914. https://doi.org/10.1134/S1070363221050224
23. J. Zhang and J. X. Li. *Z. Naturforsch. B*, **2016**, *71*, 45-49. https://doi.org/10.1515/znb-2015-0135
24. Z. Q. Hao, K. Liu, Q. Feng, Q. Dong, D. Z. Ma, Z. G. Han, G. L. Lu, and J. Lin. *Chin. J. Chem*., **2021**, *39*, 121-128. https://doi.org/10.1002/cjoc.202000363
25. Z. X. Du and J. X. Li. *Z. Naturforsch., B*, **2020**, *75*, 577-581. https://doi.org/10.1515/znb-2020-0042
26. A. J. Shubnell, E. J. Kosnic, and P. J. Squattrito. *Inorg. Chim. Acta*, **1994**, *216*, 101-112. https://doi.org/10.1016/0020-1693(93)03700-K
27. Y.-J. Liang, X. Meng, F. Huang, J. J. Guo, and Y. M. Jiang. *J. Coord. Chem*., **2011**, *64*, 3751-3757. https://doi.org/10.1080/00958972.2011.630462
28. O.-V. Dolomanov, L.-J. Bourhis, R.-J. Gildea, J. A. K. Howard, and H. J. Puschmann. *Appl. Crystallogr*., **2009**, *42*, 339-341. https://doi.org/10.1107/S0021889808042726

29. G.-M. Sheldrick. SHELXS-97: Program for crystal structure solution. Gottingen, Germany: Gottingen University, **1997**.
30. Z.-G. Gu, Y.-F. Xu, L.-C. Kang, Y.-Z. Li, J-L. Zuo, and X.-Z. You. *Inorg. Chem*., **2009**, *48*, 5073-5080. https://doi.org/10.1021/ic8023524
31. E. Elacqua, P. Kaushik, R. H. Groeneman, J. C. Sumrak, D.-K. Bucar, and L. R. MacGillivray. *Angew. Chem*., *Int. Ed*., **2012**, *51*, 1037-1041. https://doi.org/10.1002/anie.201106842
32. S. Horike, R. Matsuda, D. Tanaka, S. Matsubara, M. Mizuno, K. Endo, and S. Kitagawa. *Angew. Chem*., *Int. Ed*., **2006**, *118*, 7384-7388. https://doi.org/10.1002/ange.200603196
33. A. P. Côté and G. K. H. Shimizu. *Chem. Eur. J*., **2003**, *9*, 5361-5370. https://doi.org/10.1002/chem.200305102
34. M. Yang, S. Chen, Y.-X. Qiu, W.-B. Chen, J.-M. Lin, H. Yan, Z.-J. Ou Yang, and W. Dong. *J. Coord. Chem*., **2012**, *65*, 4255-4262. https://doi.org/10.1080/00958972.2012.736971
35. J. X. Li, T. Zhang, H. J. Chen, and Z. X. Du. *Z. Kristallogr.-Cryst. Mater.*, **2021**, *236*, 251-259. https://doi.org/10.1515/zkri-2021-2043
36. J. X. Li, L. Y. Xiong, L. L. Fu, W. B. Bo, Z. X. Du, and X. Feng. *J. Solid State Chem*., **2022**, *305*, 122636. https://doi.org/10.1016/j.jssc.2021.122636